Journal of Next Generation Technology (ISSN: 2583-021X)
Vol. 5, Issue 3, May 2025

Four Quadrant Operation and Control of Three-Phase BLDC Motor for Water Pumping Applications

Nandam Bhagy Sri[1], Sarekukka Iswarya[2], R Deeksha Raman[3],Sk.Afreen[4],
T. Narasimha Prasad[5]
[1,2,3,4]UG Scholar, [5]Associate Professor
Department of EEE, St.Ann's College of Engineering and Technology,Chirala,India
Email id : nandambhagyasri54@gmail.com, iswaryasarekukka@gmail.com, rdeeksharaman @gmail.com, afreenafreen24980@gmail.com, narasimhaiete@gmail.com

Article Received: 09 April 2025 *Article Accepted: 20 April 2025* *Article Published: 12 May 2025*

Citation
Nandam Bhagy Sri, Sarekukka Iswarya, R Deeksha Raman, Sk.Afreen, T. Narasimha Prasad, "Four Quadrant Operation and Control of Three-Phase BLDC Motor for Water Pumping Applications",Journal of Next Generation Technology(ISSN: 2583-021X), 5(3), pp. 68-81. May 2025. DOI: 10.5281/zenodo.15716067

Abstract

This study presents an efficient solar photovoltaic (SPV)-powered water pumping system utilizing a Zeta converter-fed voltage source inverter (VSI) to drive a brushless DC (BLDC) motor-pump. The system eliminates phase current sensors and minimizes switching losses by employing fundamental frequency operation of the VSI.. A hysteresis voltage control strategy ensures stable performance across varying solar irradiance levels, including low-light conditions. The Zeta converter facilitates effective maximum power point tracking (MPPT), while sensorless speed control with soft start minimizes complexity and cost. Simulation and experimental results confirm reliable MPPT, low switching losses, and robust operation, making the design ideal for off-grid agricultural use.

Keywords: SPV array, zeta converter, BLDC motor, water pumping, MPPT, hysteresis control, sensorless control, fundamental frequency switching.

I. INTRODUCTION

Utilizing solar photovoltaic (SPV)-generated electrical energy for a variety of purposes is encouraged by the sharp decline in the cost of powering modern devices and the imminence of fossil fuels. These days, water pumping—a stand-alone use of power generated by SPV arrays—is gaining a lot of attention for industrial, residential, and field irrigation. The zeta converter together with a permanent-magnet brushless dc (BLDC) motor has not yet been thoroughly investigated to create such a system, despite the fact that numerous studies have been conducted in the field of SPV array-fed water pumps, integrating different dc–dc converters and motor drives. Nevertheless, some SPV-based applications have made use of the zeta converter [1]–[3].

The zeta converter, which is a member of the buck-boost converter family, can be set to either raise or lower the output voltage. This characteristic provides an infinite range for an

SPV array's maximum power-point tracking (MPPT) [7]. If MPP falls within the specified bounds, the MPPT can be carried out using a straightforward buck [8] and boost [9] converter. Unlike a boost converter, which invariably raises the voltage level at its output without guaranteeing soft beginning, this feature also makes it easier for BLDC motors to start softly.The output current of the zeta converter is continuous, in contrast to that of a traditional buck-boost converter [10]. The output inductor eliminates ripples and maintains a constant current. In contrast to an inverting buck-boost and Cuk converter, the zeta converter functions as a non-inverting buck-boost converter, although having the same number of components as a Cuk converter [11]. This characteristic lowers the complexity and likelihood of slowing down the system response by eliminating the need for related circuits for negative voltage sensing [12]. The suggested SPV array-fed water pumping system benefits from these zeta converter advantages. The zeta converter is operated using the incremental conductance maximum power point tracking (INC-MPPT) method [8], [13]–[18] such that the SPV array always runs at its MPP. The design depicted in Fig. 3.1 serves as the foundation for the literature now available on SPV array-based BLDC motor-driven water pumps [19]–[22].

The standard method for MPPT of an SPV array is a dc–dc converter. In order to regulate the BLDC motor, two phase currents are measured in addition to feedback from Hall signals, which raises the cost. The additional control scheme, which is necessary to regulate the speed of the BLDC motor, is more expensive and complex. Furthermore, high-frequency PWM pulses are typically used to run a voltage-source inverter (VSI), which raises switching loss and lowers efficiency.

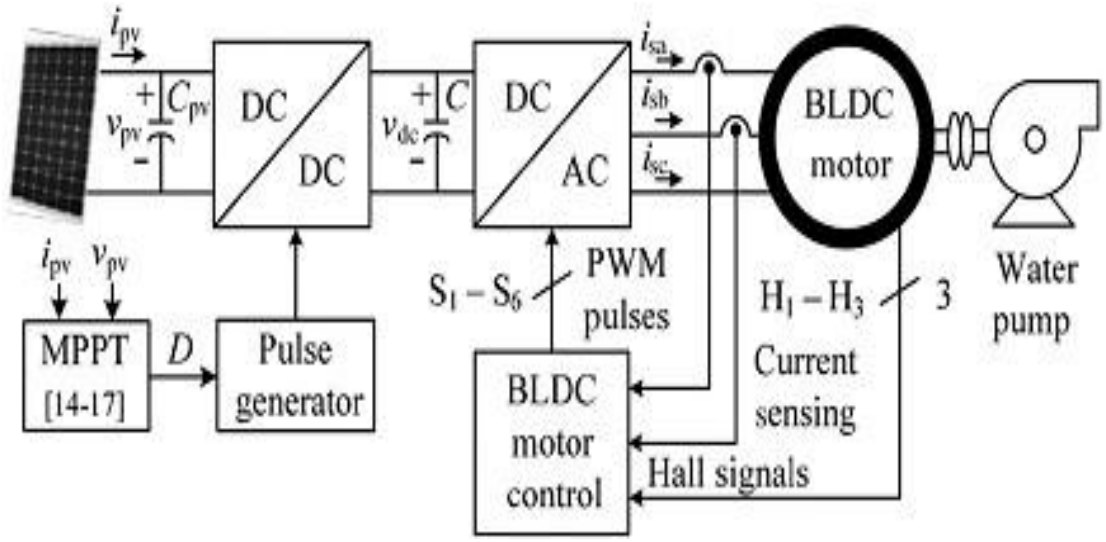

Fig 1:Conventional SPV-fed BLDC motor-driven water pumping system

Even though a Z-source inverter (ZSI) has been used to increase efficiency and lower costs in place of a conventional DC–DC converter [22], its implementation still necessitates phase current and DC-link voltage detection, which raises control complexity and system costs overall. As shown in Fig. 2, a modified SPV-fed water pumping architecture is suggested as a solution to these issues. This setup uses a Zeta converter to control the speed of a BLDC motor connected to a water pump, enable soft starting, and carry out maximum power point tracking (MPPT).The Zeta converter guarantees high efficiency, lower component stress, and a broad

MPPT operating range thanks to its single switch and continuous conduction mode (CCM) operation.

Additionally, the voltage source inverter (VSI) in the system uses fundamental frequency switching, which greatly reduces switching losses and boosts overall efficiency. Phase current and DC-link voltage sensors are removed, allowing for a more straightforward and economical design without sacrificing functionality. By varying the VSI's DC-link voltage, the BLDC motor's speed can be controlled without the use of further control systems. The MPPT algorithm's initialization process naturally achieves soft beginning. The Zeta converter and BLDC motor work together to create a small, effective, and affordable solar PV-based water pumping system. The system's dependable functioning under fluctuating solar irradiation is confirmed by MATLAB/Simulink simulation studies and experimental assessments, which show strong performance throughout startup, dynamic transitions, and steady-state settings.

II. SYSTEM DESCRIPTION

A. CONFIGURATION OF PROPOSED SYSTEMS

The suggested solar photovoltaic (SPV) array-fed water pumping system, which uses a Zeta converter to power a brushless DC (BLDC) motor, is configured as shown in Fig 2. An SPV array, Zeta converter, voltage source inverter (VSI), BLDC motor, and centrifugal water pump make up the system in that order. An encoder is included inside the BLDC motor, and the Zeta converter's switching is controlled by a pulse generator. Section II.B provides a thorough, step-by-step description of how the system works.

B. OPERATION OF PROPOSEDSYSTEM

The electrical power needed by the motor-pump system is provided by the SPV array. As shown in Fig. 2, this power is supplied to the motor-pump via a voltage source inverter (VSI) after a Zeta converter. Although the Zeta converter's power output should ideally match the input power provided by the SPV array, in practice, losses associated with the converter lead to a somewhat lower power transmission to the VSI [23]. A pulse generator that uses the incremental conductance maximum power point tracking (INC-MPPT) algorithm produces the switching pulses for the insulated gate bipolar transistor (IGBT) in the Zeta converter. This algorithm determines the ideal duty cycle to optimize power extraction by continually monitoring the voltage and current from the SPV array. The actual switching signals are generated by modulating the duty cycle against a high-frequency carrier waveform. This ensures maximum power point tracking and maximizes system efficiency. The BLDC motor, which is mechanically connected to the water pump, is powered by the voltage source inverter (VSI), which transforms the DC output from the Zeta converter into AC power. With data from its inbuilt encoder, the BLDC motor's electronic commutation makes it possible for the VSI to function via basic frequency switching. This method improves the overall efficiency of the suggested water pumping system by removing the high-frequency switching losses that are usually connected to pulse-width modulation.

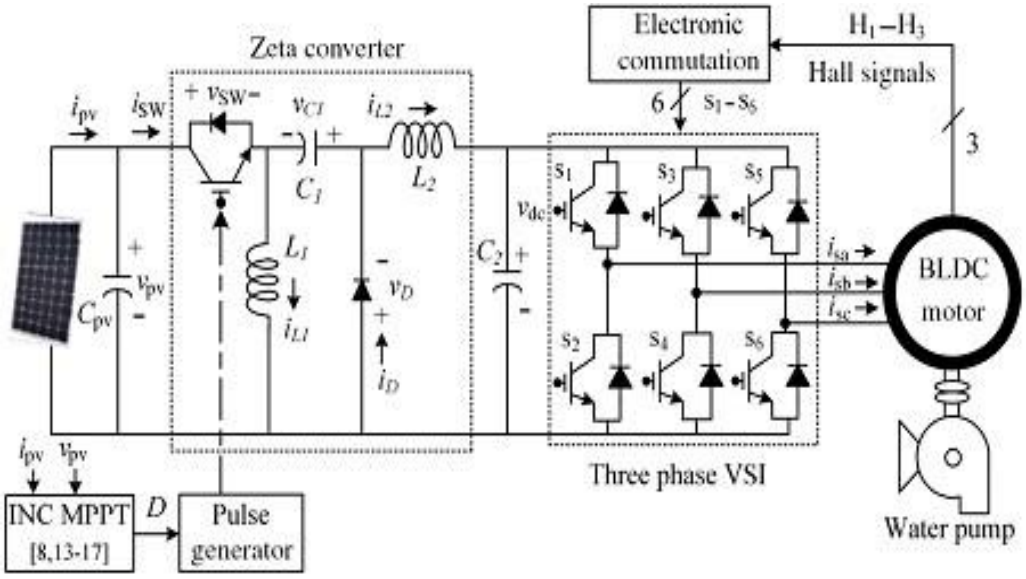

Fig 2:Proposed SPV-zeta converter-fed BLDC motor drive for water pump

III. DESIGN OF PROPOSEDSYSTEM

The operational phases depicted in Figure 3.2 have been painstakingly planned to achieve an effective water pumping system that can function dependably in a variety of unpredictable circumstances. For the system design, a solar photovoltaic (SPV) array rated at 3.4 kW peak output under standard test conditions (STC) and a brushless DC (BLDC) motor with a rated power of 2.89 kW are chosen. The following sections provide the specific design specifications and factors for the water pump, Zeta converter, and SPV array.

A. Design of SPV Array

The SPV array is purposefully larger to provide dependable operation despite these inefficiencies, taking into account the inherent power losses in practical converters as well as the mechanical and electrical losses influencing the BLDC motor-pump system. In order to overcome the motor-pump's nominal power demand, an SPV array with a peak power capacity of P_{mpp}= 3.4 under standard test circumstances (STC: 1000 W/m² irradiance, 25°C temperature, AM 1.5) is chosen. The Solar World Sun module Plus SW 280 mono photovoltaic module [24] served as the model for the array design. Table 3.1 provides a summary of the electrical specs for the module. Using V_{mpp} = 187.2 as the maximum power point under STC, the number of modules connected in series and parallel is calculated to reach the specified array voltage.

B. Table 1: *Specifications of Sun module plus SW 280 mono SPV Module*

Peak power, P_m (W)	280
Open circuit voltage, V_o (V)	39.5
Voltage at MPP, V_m (V)	31.2
Short circuit current, I_s (A)	9.71
Current at MPP, I_m (A)	9.07
Number of cells connected in series, N_{ss}	60

The current of SPV array at MPP I_{mpp} is estimated as

$$I_{mpp} = P_{mpp}/V_{mpp} = 3400/187.2 = 18.16A \quad (1)$$

The numbers of modules required to connect in series are as follows:

$$N_s = V_{mpp}/V_m = 187.2/31.2 = 6 \quad (2)$$

The numbers of modules required to connect in parallel are as follows:

$$N_s = V_{mpp}/V_m = 187.2/31.2 = 6 \quad (3)$$

$$N_p = I_{mpp}/I_m = 18.16/9.07 = 2 \quad (4)$$

Six photovoltaic modules are connected in series per string, with two of these strings set up in parallel, to meet the required electrical standards. An SPV array of the right size for the suggested system is produced by this configuration.

C. Design of Zeta Converter

The Zeta converter is the next step in the suggested system after the SPV array. Important parts of its design include the estimation of the intermediate capacitor (C_1), output inductor (L_2), and input inductor (L_1). In order to minimize electrical stress on the converter's electronics and improve overall reliability, these components are dimensioned to assure continuous conduction mode (CCM) operation. The duty cycle (D), the fundamental parameter for scaling the converter parts, is estimated at the start of the design process. The following formula is used to determine the initial duty cycle [6]:

$$D = \frac{V_{dc}}{(V_{dc}+V_{mpp})} = 200/(200 + 187.2) = 0.52 \quad (5)$$

The average output voltage of the Zeta converter, which also acts as the DC link voltage for the VSI, is denoted here by Vdc. To guarantee optimum performance, this voltage is set to match the BLDC motor's rated DC voltage.

An average current flowing through the dc link of the VSI I_{dc} is estimated as

$$I_{dc} = \frac{P_{mpp}}{V_{dc}} = \frac{3400}{200} = 17A \quad (6)$$

Then, L1, L2, and C1 are estimated as

$$L_1 = \frac{DV_{mpp}}{F_{sw}\Delta I_{L1}} = \frac{0.52X187.2}{20000X18.16X0.06} = 4.5x10^{-3} \quad (7)$$

$$L_2 = \frac{(1-D)V_{DC}}{F_{sw}\Delta I_{L2}} = \frac{(1-0.52)X200}{20000X17X0.06} = 4.7X10^{-3} \quad (8)$$

$$C_1 = \frac{DI_{dc}}{F_{sw}\Delta V_{C1}} = \frac{0.52X17}{20000X200X0.1} = 2210^{-6}F \quad (9)$$

Here, f_{sw} represents the IGBT switch's switching frequency in the Zeta converter. The permissible ripple current in the input inductor L_1 is denoted by ΔI_{L1}. This current is assumed to be equal to the array current at maximum power point, or $I_{L1} = I_{mpp}$. Similarly, the allowed ripple current in the output inductor $L_2$is represented as ΔI_{L2}, which is considered to be equal to the DC link current, $I_{L2} = I_{dc}$. The permissible ripple voltage across the intermediate capacitor C_1 is indicated by ΔV_{C1}, which is assumed to be equal to the DC link voltage, or $V_{C1} = V_{dc}$.

D. Estimation of DC-Link Capacitor of VSI

The voltage source inverter's (VSI) DC-link capacitor is estimated using a revolutionary design methodology. This method is based on the idea that the primary harmonic distortion in a three-phase supply system is the sixth harmonic component of the AC output voltage, which is strongly mirrored on the DC side [25]. As a result, the rated and minimum operating speeds of the BLDC motor needed for efficient water pumping are used to calculate the VSI's fundamental output frequencies. The corresponding capacitor values are then calculated using these frequencies. The bigger of the two anticipated capacitor values is chosen to provide dependable system functioning under a range of solar irradiance situations, especially at low irradiance levels.

$$\omega_{rated} = 2\pi \frac{N_{rated}P}{120} = 2\pi \frac{3000X6}{120} = 942rad/s \quad (10)$$

The fundamental output frequency of the VSI corresponding to the minimum operating speed of the BLDC motor—necessary to sustain effective water pumping—is used as a critical parameter in the estimation of the minimum required DC-link capacitance. (N= 1100r/min) ω_{min} is estimated as

$$\omega_{min} = 2\pi f_{min} = 2\pi \frac{NP}{120} = 345.57rad/s \quad (11)$$

Here, f_{rated} and f_{min} represent the fundamental output frequencies of the VSI corresponding to the rated speed and the minimum speed of the BLDC motor required for effective water pumping, respectively, and are expressed in hertz (Hz). N_{rated} denotes the rated speed of the BLDC motor in revolutions per minute (rpm), and PPP is the number of poles of the motor. The value of dc link capacitor of VSI at ω_{rated} is as follows:

$$C_{2,rated} = \frac{I_{dc}}{6X\omega_{min}X\Delta V_{dc}} = \frac{17}{6X942X200X0.1} = 150.4\mu F \quad (12)$$

Similarly, a value of dc link capacitor of VSI at ω_{min} is as follows:

$$C_{2,min} = \frac{I_{dc}}{6X\omega_{min}X\Delta V_{dc}} = \frac{17}{6X345.57X200X0.1} = 410\mu F \quad (13)$$

Where ΔVdc is an amount of permitted ripple in voltage across dc-link capacitor C2. Finally, C2= 410μF is selected to design the dc-link capacitor.

E. Design of Water Pump

To determine the proportionality constant K for the selected water pump, its power–speed characteristic is utilized, as described in references, and is expressed as:

$$K = \frac{P}{\omega_r^3} = \frac{2.89X10^{-3}}{2\pi X3000/60^3} = 9.32X10^{-5} \quad (14)$$

In this case, \omega_r is the rated mechanical angular speed of the rotor, which is equivalent to 3000 revolutions per minute (rpm), expressed in radians per second, and P=2.89 kWP = 2.89 indicates the rated mechanical power provided by the BLDC motor. A water pump that satisfies these requirements is chosen to be incorporated into the suggested system.

Table 2: Switching States for Electronic Commutation of BLDC Motor

Rotor position θ (°)	Hall signals			Switching states					
	H_3	H_2	H_1	S_1	S_2	S_3	S_4	S_5	S_6
NA	0	0	0	0	0	0	0	0	0
0–60	1	0	1	1	0	0	1	0	0
60–120	0	0	1	1	0	0	0	0	1
120–180	0	1	1	0	0	1	0	0	1
180–240	0	1	0	0	1	1	0	0	0
240–300	1	1	0	0	1	0	0	1	0
300–360	1	0	0	0	0	0	1	1	0
NA	1	1	1	0	0	0	0	0	0

IV. CONTROL OF PROPOSED SYSTEM

The proposed system is controlled in two stages. These two control techniques, viz., MPPT and electronic commutation, are discussed as follows.

A. INC-MPPT Algorithm

To maximize power extraction from the SPV array and allow for soft starting of the BLDC motor, an effective and popular incremental conductance (INC) maximum power point tracking (MPPT) technique is used [8], [13]. This technique allows for variations in the converter's duty cycle or the SPV array voltage. The complexity of the system is increased when the array voltage is perturbed since a proportional-integral (PI) controller is usually required to calculate the correct duty cycle [8]. In the current work, a direct duty cycle control technique is used to prevent this. The INC-MPPT algorithm uses the slope of the $P_{pv} -$ $_{pv}$ characteristic curve to identify the proper perturbation direction.

. The principle is as follows: the slope is zero at the maximum power point (MPP), positive to the left of the MPP, and negative to the right of the MPP, i.e.,

$$\left.\begin{aligned} \frac{dP_{\text{pv}}}{dv_{\text{pv}}} &= 0; \quad \text{at mpp} \\ \frac{dP_{\text{pv}}}{dv_{\text{pv}}} &> 0; \quad \text{left of mpp} \\ \frac{dP_{\text{pv}}}{dv_{\text{pv}}} &> 0; \quad \text{right of mpp} \end{aligned}\right\} \tag{15}$$

Since

$$\frac{dP_{\text{pv}}}{dv_{\text{pv}}} = \frac{d(v_{\text{pv}} * i_{\text{pv}})}{dv_{\text{pv}}} = i_{\text{pv}} + v_{\text{pv}} * \frac{di_{\text{pv}}}{dv_{\text{pv}}} \cong i_{\text{pv}} + v_{\text{pv}} * \frac{\Delta i_{\text{pv}}}{\Delta v_{\text{pv}}} \tag{16}$$

Therefore, (3.14) is rewritten as

$$\left.\begin{aligned} \frac{\Delta i_{pv}}{\Delta v_{pv}} &= -\frac{i_{pv}}{v_{pv}}; && \text{at mpp} \\ \frac{\Delta i_{pv}}{\Delta v_{pv}} &> -\frac{i_{pv}}{v_{pv}}; && \text{left of mpp} \\ \frac{\Delta i_{pv}}{\Delta v_{pv}} &< -\frac{i_{pv}}{v_{pv}}; && \text{right of mpp} \end{aligned}\right\} \quad (17)$$

As shown in Fig. 3, the controller detects the direction of duty cycle perturbation by comparing the relationship between incremental conductance and instantaneous conductance, and then modifies the duty cycle accordingly. For instance, the duty cycle is gradually raised by a predetermined step size when operating to the right of the MPP until the perturbation direction reverses. Although the perturbation should ideally stop when it reaches the MPP, in real-world situations, the operating point fluctuates around the MPP. The tracking time to reach the MPP is extended when the perturbation step size is decreased, while oscillations are reduced. In order to meet the dual goals of effective MPPT and smooth soft starting of the BLDC motor, a careful trade-off between tracking speed and perturbation magnitude is made.

The duty cycle is set to zero to enable gentle beginning, and an ideal perturbation step size of ΔD=0.001\Delta D = 0.001ΔD=0.001 is used to minimize oscillations and guarantee fast tracking performance.

B. Electronic Commutation of BLDC Motor

A voltage source inverter (VSI) that uses electronic commutation controls the BLDC motor. With electronic commutation, decoder logic is used to successively change the motor winding currents based on the rotor position. For a 120° conduction interval, this method symmetrically aligns the DC input current in the center of each phase voltage. Three Hall-effect sensor signals, which are obtained from the motor's integrated encoder and correspond to the rotor position, can be combined to create six switching pulses. Every unique combination of Hall signals, separated by 60° intervals, corresponds to a particular range of rotor positions [5, 6].

V. RESULTS & DISCUSSION

The Simulink diagram shown in Fig 3 depicts the schematic of the suggested system, a solar PV-fed BLDC motor-driven water pumping system. It is powered by PWM produced by the MPPT control method and is fed by solar PV and a DC-DC converter. A three-phase inverter is linked to the DC-DC converter's output. Additionally, this three-phase inverter feeds a BLDC motor. In order to pump water, the pump is coupled to a BLDC motor. and the BLDC Simulink model is used to simulate it by providing mechanical torque as an input. The suggested SPV array-based zeta converter-fed BLDC motor drive for water pump's starting and steady-state performances are shown in Fig. 4.

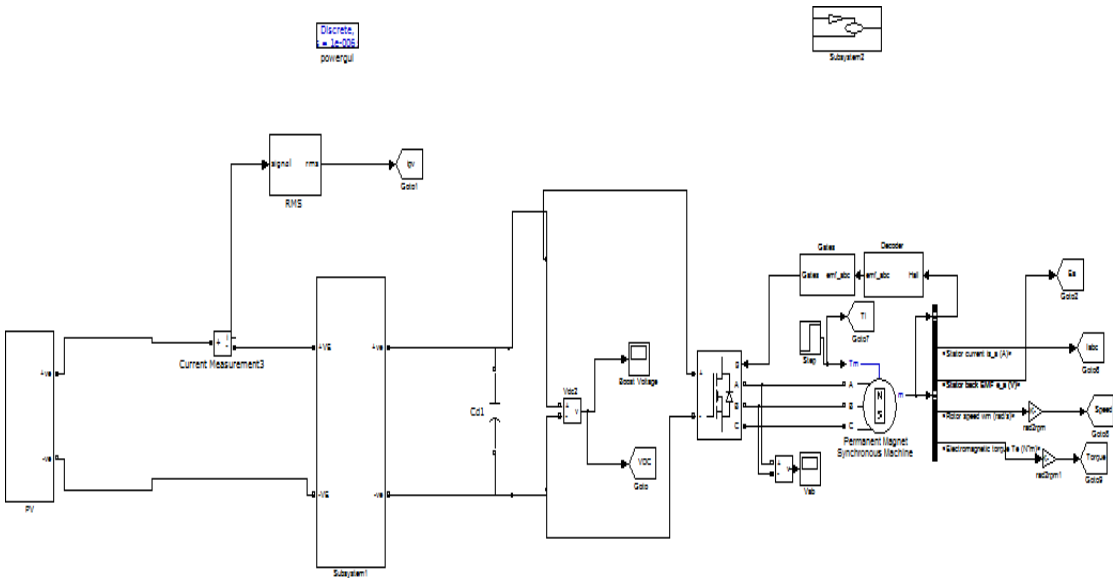

Fig 3: Simulation circuit Conventional SPV-fed BLDC motor-driven water pumping system

Figure 4(a) illustrates the voltage, current, and power waveforms of the solar PV array variables. Figure 4(b) presents the Zeta converter variables, including voltages and currents across the inductors and capacitor, as well as input and output parameters. Figure 4(c) depicts the BLDC motor-pump variables, such as stator and rotor currents, input voltage, load torque, and motor speed.

Figure 5 depicts the Simulink model of the conventional SPV-fed BLDC motor-driven water pumping system incorporating a speed controller. Figure 6 illustrates the starting and steady-state performance characteristics of the proposed SPV array-based, zeta converter-fed BLDC motor-pump system utilizing a hysteresis voltage controller.

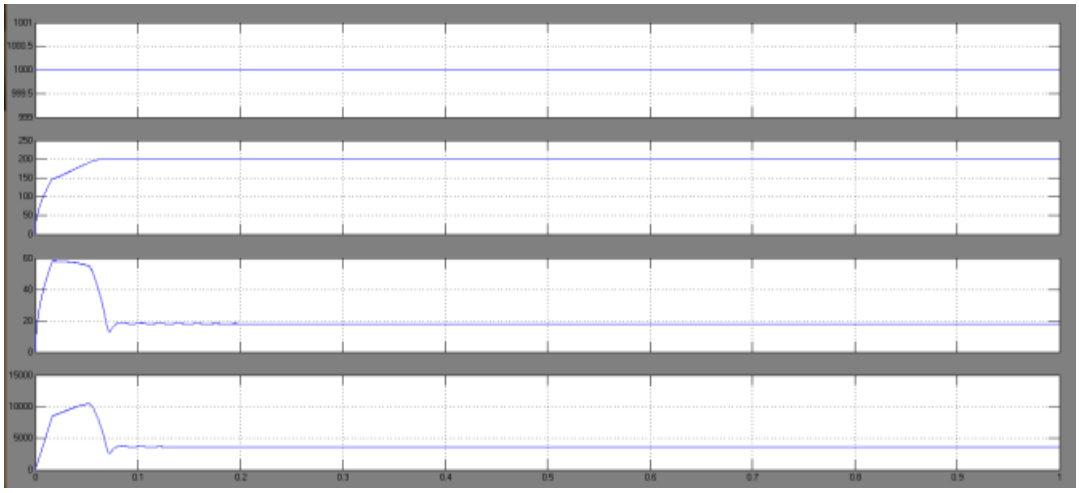

(a)

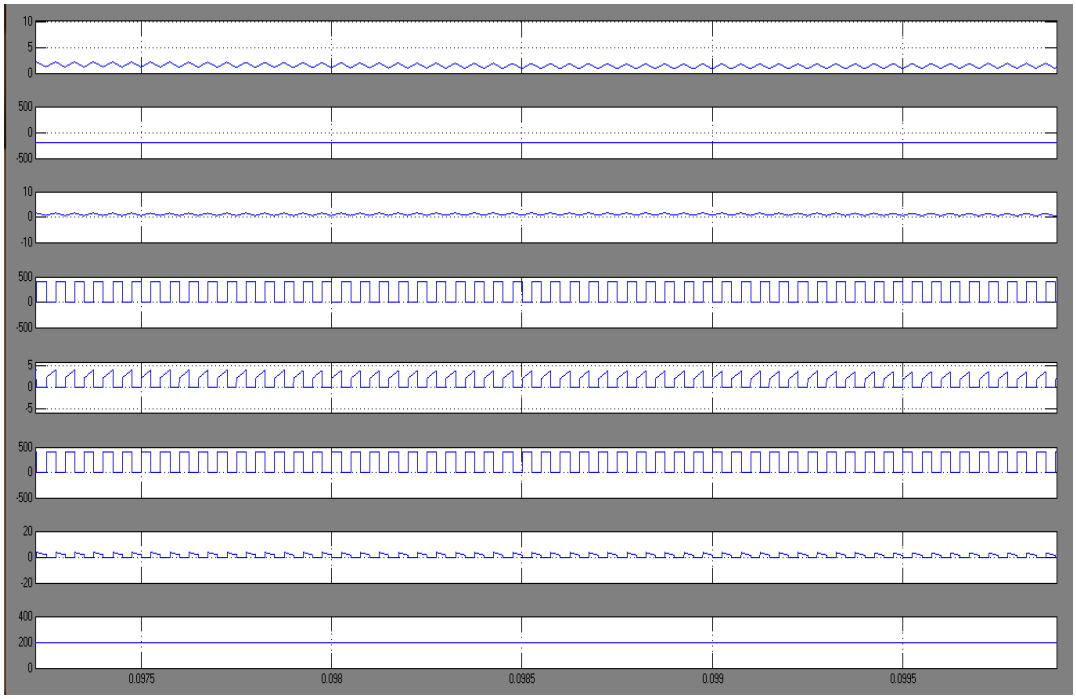

(b)

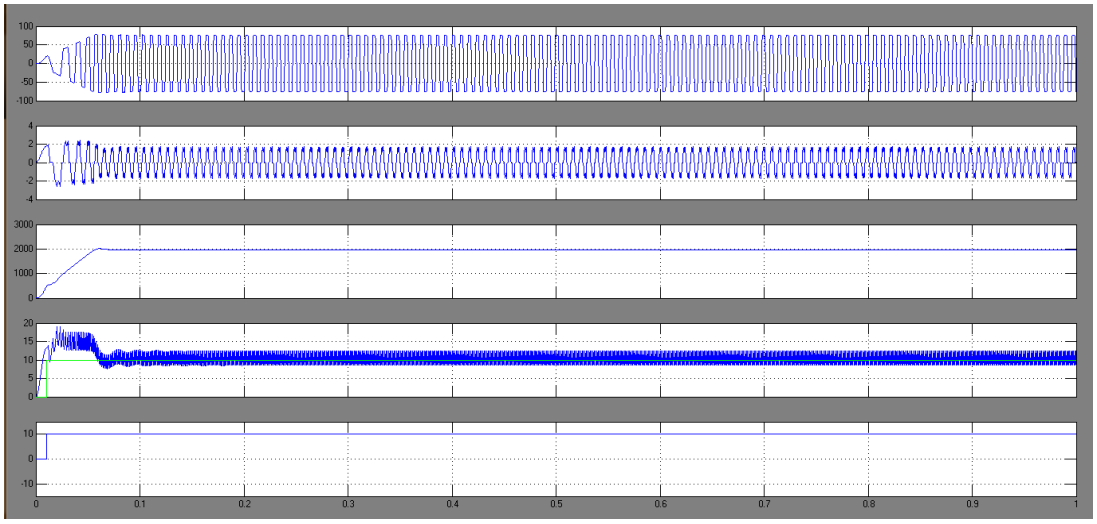

(c)

Fig 4:Starting and steady-state performances of the proposed SPV array based zeta converter- fed BLDC motor drive for water pump. (a) SPV array variables. (b) Zeta converter variables. (c) BLDC motor-pump variables

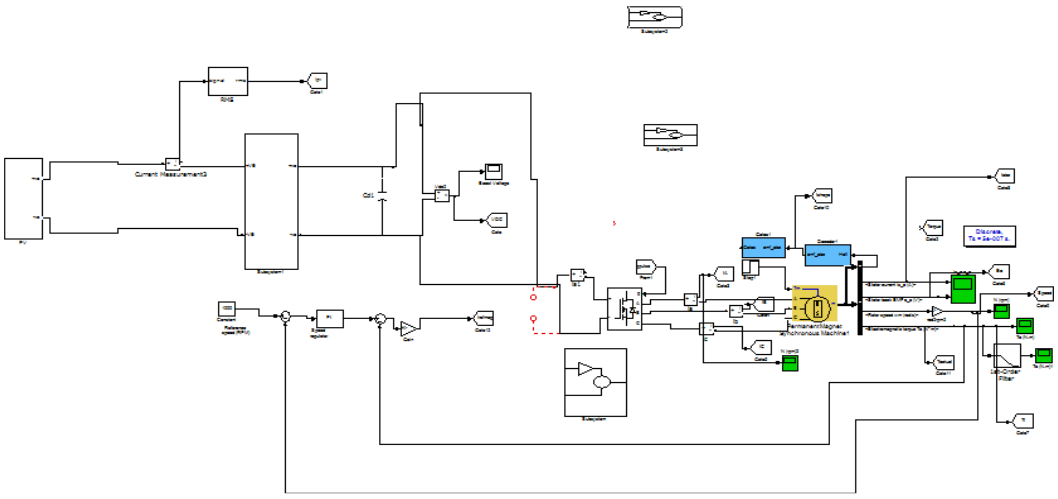

Fig 5: simulation circuit Conventional SPV-fed BLDC motor-driven water pumping system with speed controller

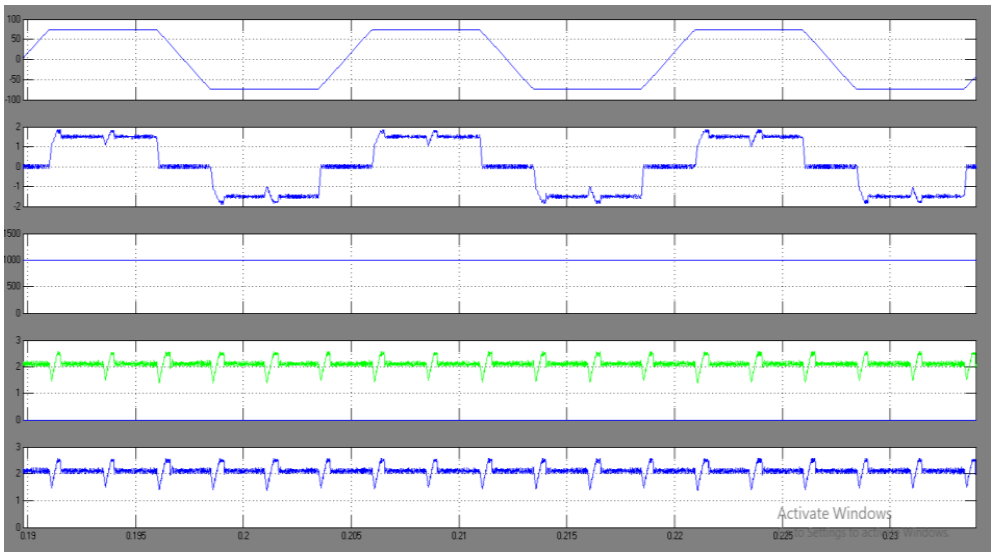

Fig 6: Starting and steady-state performances of the proposed SPV array based zeta converter- fed BLDC motor-pump variables with hysteresis voltage controller

VI. CONCLUSION

A zeta converter-fed VSI and a BLDC motor are used in a proposed solar photovoltaic (SPV) array-driven water pumping system, and extensive simulation has shown how effective it is. The system's performance was evaluated in starting, dynamic, and steady-state scenarios after it was painstakingly built and modelled to meet important operational goals. The assessment validates the beneficial combination of the BLDC motor and zeta converter for SPV-based water pumping applications. The VSI's fundamental frequency switching, which drastically lowers switching losses, the BLDC motor's smooth soft-starting, and the SPV array's effective maximum power point tracking are among the key functionalities attained. Furthermore, the method reduces cost and system complexity by removing the need for phase current and DC-link voltage sensors and enabling BLDC motor speed control without the need for auxiliary controllers. Even in situations with low solar irradiation, the suggested setup, which was managed by a hysteresis voltage method, showed strong performance.

References

[1]. M. Uno and A. Kukita, "Single-switch voltage equalizer using multi stacked buck–boost converters for partially-shaded photovoltaic modules," IEEE Trans. Power Electron., vol. 30, no. 6, pp. 3091–3105, Jun. 2015.

[2]. R. Arulmurugan and N. Suthanthiravanitha, "Model and design of a fuzzy-based Hopfield NN tracking controller for standalone PV applications," Elect. Power Syst. Res., vol. 120, pp. 184– 193, Mar. 2015.

[3]. S. Satapathy, K. M. Dash, and B. C. Babu, "Variable step size MPPT algorithm for photo voltaic array using zeta converter—A comparative analysis," in Proc. Students Conf. Eng. Syst. (SCES), Apr. 12–14, 2013, pp. 1–6.

[4]. R. Kumar and B. Singh, "BLDC motor driven solar PV array fed water pumping system employing zeta converter," in Proc. 6th IEEE India Int. Conf. Power Electron. (IICPE), Dec. 8– 10, 2014, pp. 1–6.

[5]. B. Singh, V. Bist, A. Chandra, and K. Al-Haddad, "Power factor correction in bridgeless-Luo converter-fed BLDC motor drive," IEEE Trans. Ind. Appl., vol. 51, no. 2, pp. 1179–1188, Mar./Apr. 2015.

[6]. B. Singh and V. Bist, "Power quality improvements in a zeta converter for brushless dc motor drives," IET Sci. Meas. Technol., vol. 9, no. 3, pp. 351–361, May 2015.

[7]. R. F. Coelho, W. M. dos Santos, and D. C. Martins, "Influence of power converters on PV maximum power point tracking efficiency," in Proc. 10th IEEE/IAS Int. Conf. Ind. Appl. (INDUSCON), Nov. 5–7, 2012, pp. 1–8.

[8]. M. A. Elgendy, B. Zahawi, and D. J. Atkinson, "Assessment of the incremental conductance maximum power point tracking algorithm," IEEE Trans. Sustain. Energy, vol. 4, no. 1, pp. 108– 117, Jan. 2013.

[9]. M. Sitbon, S. Schacham, and A. Kuperman, "Disturbance observer based voltage regulation of current-mode-boost-converter-interfaced photovoltaic generator," IEEE Trans. Ind. Electron., vol. 62, no. 9, pp. 5776– 5785, Sep. 2015.

[10]. R. Kumar and B. Singh, "Buck–boost converter fed BLDC motor drive for solar PV array based water pumping," in Proc. IEEE Int. Conf. Power Electron. Drives Energy Syst. (PEDES), Dec. 16–19, 2014, pp. 1–6.

[11]. A. H. El Khateb, N. Abd. Rahim, J. Selvaraj, and B. W. Williams, "DC to-dc converter with low input current ripple for maximum photovoltaic power extraction," IEEE Trans. Ind. Electron., vol. 62, no. 4, pp. 2246– 2256, Apr. 2015.

[12]. D. D. C. Lu and Q. N. Nguyen, "A photovoltaic panel emulator using a buck–boost dc/dc converter and a low cost micro-controller," Solar Energy, vol. 86, no. 5, pp. 1477–1484, May 2012.

[13]. Z. Xuesong, S. Daichun, M. Youjie, and C. Deshu, "The simulation and design for MPPT of PV system based on incremental conductance method," in Proc. WASE Int. Conf. Inf. Eng. (ICIE), Aug. 14–15, 2010, vol. 2, pp. 314–317.

[14]. A. R. Reisi, M. H. Moradi, and S. Jamasb, "Classification and comparison of maximum power point tracking techniques for photovoltaic system: A review," Renew. Sustain. Energy Rev., vol. 19, pp. 433–443, Mar. 2013.

[15]. B. Bendib, H. Belmili, and F. Krim, "A survey of the most used MPPT methods: Conventional and advanced algorithms applied for photovoltaic systems," Renew. Sustain. Energy Rev., vol. 45, pp. 637–648, May 2015.

[16]. B. Subudhi and R. Pradhan, "A comparative study on maximum power point tracking techniques for photovoltaic power systems," IEEE Trans.Sustain. Energy, vol. 4, no. 1, pp. 89–98, Jan. 2013.

[17]. M. A. G. de Brito, L. Galotto, L. P. Sampaio, G. de Azevedo e Melo, and C. A. Canesin, "Evaluation of the main MPPT techniques for photovoltaic applications," IEEE Trans. Ind. Electron., vol. 60, no. 3, pp. 1156–1167, Mar. 2013.

[18]. K. S. Tey and S. Mekhilef, "Modified incremental conductance algorithm for photovoltaic system under partial shading conditions and load variation," IEEE Trans. Ind. Electron., vol. 61, no. 10, pp. 5384–5392, Oct. 2014.

[19]. M. Ouada, M. S. Meridjet, and N. Talbi, "Optimization photovoltaic pumping system based BLDC using fuzzy logic MPPT control," in Proc. Int. Renew. Sustain. Energy Conf. (IRSEC), Mar. 7–9, 2013, pp. 27–31.

[20]. M. Dursun and S. Ozden, "Application of solar powered automatic water pumping in Turkey," Int. J. Comput. Elect. Eng., vol. 4, no. 2, pp. 161– 164, 2012.

[21]. Gnanavel, C., Immanuel, T.B., Muthukumar, P., Lekshmi Kanthan, P.S. (2018). Investigation on Four Quadrant Operation of BLDC MOTOR Using Spartan-6 FPGA. In: Zelinka, I., Senkerik, R., Panda, G., Lekshmi Kanthan, P. (eds) Soft Computing Systems. ICSCS 2018.

[22]. Anuradha, K. & Erlaally, Deekshitha & Karuna, G. & Srilakshmi, V. & Adilakshmi, K.. (2021). Analysis Of Solar Power Generation Forecasting Using Machine Learning Techniques. E3S Web of Conferences. 309. 01163. 10.1051/e3sconf/202130901163

[23]. Immanuel, T & Paramasivan, Muthukumar & Gnanavel, C. & Muthaiyan, Rajavelan & Marimuthu, M.. (2018). Transformer less 1Φ Inverter for Grid-Connected PV Systems with an Optimized Control. International Journal of Engineering and Technology(UAE). 7. 217-220. 10.14419/ijet.v7i3.34.18968.

[24]. Gnanavel, C., Immanuel, T.B., Muthukumar, P., Lekshmi Kanthan, P.S. (2018). Investigation on Four Quadrant Operation of BLDC MOTOR Using Spartan-6 FPGA. In: Zelinka, I., Senkerik, R., Panda, G., Lekshmi Kanthan, P. (eds) Soft Computing Systems. ICSCS 2018. Communications in Computer and Information Science, vol 837. Springer, Singapore. https://doi.org/10.1007/978-981-13-1936-5_77

[25]. S. Benisha, J. A. Roseline, K. Murugesan, D. Lakshmi, G. Ezhilarasi and P. Muthukumar, "Enrichment in power quality using Power Factor Correction Cuk converter fed BLDC Motor Drive," *2023 9th International Conference on Electrical Energy Systems (ICEES)*, Chennai, India, 2023, pp. 590-598, doi: 10.1109/ICEES57979.2023.10110134.

[26]. M. Paramasivan, V. Nagarajan, L. Padmasuresh and M. V. Suganyadevi, "Power Factor Correction Strategies for BLDC Drives – A Review," *2022 Third International Conference on Intelligent Computing Instrumentation and Control Technologies (ICICICT)*, Kannur, India, 2022, pp. 1821-1826, doi: 10.1109/ICICICT54557.2022.9917783.